



Preparation and Characterization of Desensitized ϵ -HNIW in Solvent-Antisolvent Recrystallizations

Xiabing JIANG*, Xueyong GUO*, Hui REN and Qingjie JIAO

*State Key Laboratory of Explosion Science and Technology,
Beijing Institute of Technology, Beijing, 100081, China*

**E-mail: nust@bit.edu.cn, jiangxb13@163.com*

Abstract: The solubility of hexanitrohexaazaisowurtzitane (HNIW) in solvent and solvent-antisolvent mixtures, and the temperature at which the HNIW's polymorph transforms were studied. The solubility of HNIW in solvent-antisolvent mixtures was measured at 30 °C and these data were fitted to a generalized solubility curve. Recrystallization experiments were conducted at 30 °C in the case of saturation with the volume ratio of ethyl acetate to petroleum ether (chloroform) ranging from 0:1 to 4:1. Desensitized HNIW was obtained by ethyl acetate and petroleum ether crystallization and characterized by Fourier Transform Infrared Spectroscopy (FTIR), X-ray Diffraction (XRD), High Performance Liquid Chromatography (HPLC) and Scanning Electron Microscopy (SEM). The FTIR and XRD spectra confirmed the structural features of ϵ -HNIW. The blocklike ϵ -HNIW grains had an average particle size of 160 μm and high purity (98.52%). The decomposition of ϵ -HNIW was observed in the temperature range of 225-246 °C by Differential Scanning Calorimetry (DSC). Furthermore, the impact and friction sensitivity tests suggested that the desensitized ϵ -HNIW was less sensitive than raw HNIW. Small scale gap tests with desensitized ϵ -HNIW showed that these crystals are less sensitive to shock initiation.

Keywords: ϵ -HNIW, supersaturation, crystal morphology, thermal decomposition, reduced sensitivity

Introduction

2,4,6,8,10,12-Hexanitro-2,4,6,8,10,12-hexaazaisowurtzitane, commonly called HNIW, is a novel, high-density, cyclic nitramine, which can be used as an energetic component in propellant and explosives formulations [1]. It meets

stringent munitions sensitivity requirements and has a higher energy content than cyclotetramethylenetetranitramine (HMX) and cyclotrimethylenetrinitramine (RDX) which are conventionally used. HNIW is a next generation, highly energetic material (HEM). Of great interest are its high density (2.04 g/cm^3) due to the cage structure, and a standard molar enthalpy of formation of the order of about 419 kJ/mol . This is attributed to the typical structural features, including ring strain. HNIW is envisaged to deliver 14% to 20% higher performance than HMX [2, 3]. Its superior performance potential, relative to HMX, emanates not only from its much higher standard enthalpy of formation (ΔH_f°) but also from its relatively superior oxygen balance. It has been a laboratory curiosity for a long time. The production technology elaborated by Thiokol Corporation, USA, and SNPE, France, resulted in its emergence as a commercially viable, superior alternative to HMX [4, 5]. However, it has high impact and friction sensitivity which are close to those of pentaerythritol tetranitrate (PETN). Therefore, controlling the crystal density and lowering the mechanical sensitivity of HNIW have attracted a great deal of attention in order to produce insensitive HEMs.

There are four polymorphs (α -, β -, γ -, and ε -forms) of HNIW crystals. The α - and β -forms of the crystals have the space groups of $Pbca$ and $Pb2_1a$, respectively, and the γ - and ε -HNIW crystals have the same space group of $P2_1/n$. α -HNIW always exists as the hydrate form. Among the four crystal forms, the ε -form is the most stable thermodynamically and mechanically due to its highly symmetric molecular configuration, which also provides better density, solubility, and thermal stability compared with the other forms (α , β , and γ). According to the report of Foltz et al., the β -form can be transformed into the γ -form and then finally into the ε -form by adjusting the solvent and temperature of the recrystallization [6, 7]. Along with the structural transformation, the crystal density is shifted from 1.98 g/cm^3 (β -form) to 2.044 g/cm^3 (ε -form). As far as is known, the impact, friction and shock sensitivities of HNIW are influenced by void defects in the crystal structure, particle size and distribution, and the crystal morphology. When crystal growth was promoted during recrystallization, the crystal density was found to deviate from the theoretical density, probably due to the inclusion of voids in the crystals that amplified the decrease in the crystal density. On the basis of spray-crystal refinement, Sivabalan, Mohan and Yadollah found that refining the particle size of HNIW to the micro/nano scale with a narrow size distribution, results in a lower mechanical sensitivity than that of the raw material [8-10]. However, an ultrafine powder of HNIW with various polymorphs and irregular shapes would be restricted in applications in mixed explosives due to agglomeration among particles. For this reason, Myung-Ho has obtained ε -HNIW grains with high densities ranging from

1.97 g/cm³ to 2.05 g/cm³ by slow evaporative crystallization that has been shown to affect sensitivity and performance [11]. Meanwhile, as with crystallization of RDX, Borne observed that the inclusion of void defects in the crystal structure reduced the crystal density and shock insensitivity of the explosive formulation [12]. Reduced Sensitivity-RDX (RS-RDX) was first developed by SNPE and subsequently similar research was imitated by Bui-Dang and Oxley [13-15].

Although previous studies have indicated that the properties and performance of HNIW are dictated by the polymorph and molecular structure, thus controlling the crystal density, reducing the mechanical sensitivity in the course of recrystallization has not been extensively studied. Consequently, this study investigated desensitization of HNIW via its controlled recrystallization.

Experiments

Materials

Raw HNIW was obtained from Qingyang Chemical Industry Corporation, Liaoning Province. Its crystal morphology and particle size are shown in Figure 1.

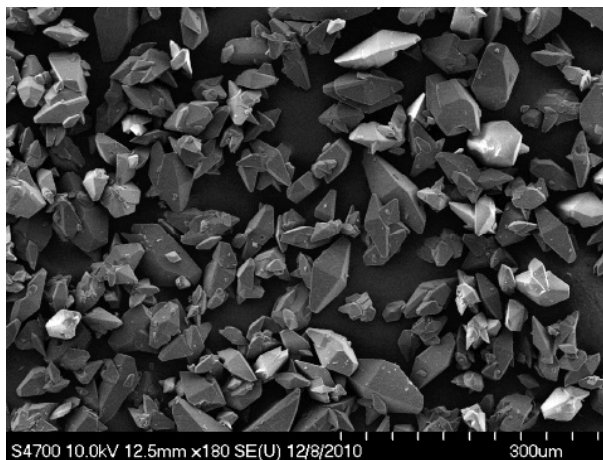


Figure 1. SEM image of raw HNIW.

The bulk density was measured by its flotation density in a graduated cylinder filled with water according to Archimedes principle. Raw HNIW had a bulk density of 0.94 g/cm³, an average particle size of 100 μ m, and was poorly free flowing in the form of loose spindle shaped, agglomerated-crystals (major β -form). The shapes were similar to those in Ref. [6]. It had a wide size

distribution and high impact and friction sensitivity. The melting point of HNIW was lower than that of HMX, i.e. approximately 240 °C.

Solubility of HNIW

Raw HNIW was dissolved in ethyl acetate (AR grade, Tianjin) at 30 °C to form a saturated solution. An equal volume of petroleum ether (AR grade, boiling range from 90-120 °C, Tianjin) or chloroform (trichloromethane) (AR grade, Tianjin) was then added to crystallize-out the HNIW. Hence, the solubility of HNIW in the solvent and antisolvent was obtained, and the HNIW crystals were purified by recrystallization.

According to the solubility of HNIW, the weight ratio of HNIW to ethyl acetate was fixed at 1:2, and then the volume ratio of ethyl acetate to petroleum ether (chloroform) was fixed at 0:1, 1:1, 1.4:1, 2:1, 3:1 and 4:1, respectively. The antisolvent should be added to the solvent at a slow rate with a stirring rate of 100-150 rpm. After continuous stirring for several hours, the resulting crystals were filtered off and dried in a desiccator at 50 °C before use. The solubility of HNIW in the solvent and the solvent-antisolvent mixtures was obtained.

General methods

The solvent and antisolvent recrystallization was used to control the morphology and density of the ϵ -HNIW crystals. Initially, 10 g raw HNIW powder was completely dissolved in 22 ml of ethyl acetate in a vial of 250 ml capacity, which was then placed in a water bath. The temperature was accurately fixed at 30 \pm 0.1 °C. About 80 ml of petroleum ether was added at a uniform rate through a circular arc pipe with diameter 1.65 mm using a constant flow pump over a period of 2 h. During recrystallization, the temperature was maintained at 30 \pm 0.1 °C to prevent any temperature effects on the recrystallization and the stirring rate was at 100-150 rpm. When bright HNIW needles had separated out from the mother liquor, the stirrer was stopped and the grains were filtered off, and dried to obtain 8 g of HNIW with good flowability and a bulk density of 1.10 g/cm³. The remaining HNIW was evaporated out from mother liquor at 50 °C.

The structure and density of HNIW and the single crystals resulting from the evaporation recrystallization were analyzed by Fourier transform infrared spectroscopy and pycnometry. The structural features of ϵ -HNIW were confirmed by Fourier transform infrared spectroscopy (VERTEX70 BRUKER Germany) using KBr pellets. X-ray diffraction (XRD) data were recorded on a D/max 2500 (Japan, Rigaku) diffractometer with monochromatized Cu K α radiation at 40 kV and 40 mA. Samples were packed into a vitreous holder and scanned from 2 to 50° 2 θ , increasing at a step size of 0.02° every second. Particle size analysis was

performed on a MASTERSIZER 2000 analyzer of measurement range from 2 to 2000 μm (UK). The crystal morphologies were examined by S-4700 Scanning electron microscope (SEM) instrument (Japan, Hitachi) at 1.0 kV and 10 μA . The purity of ϵ -HNIW was determined by LC3000 high performance liquid chromatography (HPLC) with a C18 column, and a mobile phase consisting of acetonitrile-water (volume ratio 60:40). The differential scanning calorimetric (DSC) analysis was recorded on a DSC (NETZSCH STA449C Germany) instrument by heating 0.92 mg raw HNIW and 0.88 mg ϵ -HNIW samples at a rate of 5 K/min in a nitrogen atmosphere (50 ml/min). A ZBL-B and 12 TOOL impact instruments were used to test the impact sensitivity of ϵ -HNIW, and each sample was tested 35 times (30 mg per test) to obtain a H_{50} (drop-height of 50% explosion probability) with a 5000 g drop weight. A WM-1 friction instrument ($90 \pm 1^\circ$, 3.92 MPa) was employed to test the friction sensitivity of the samples, each sample was tested 25 times (20 mg per test) and an explosion probability (P %) was obtained. A small scale gap test (SSGT) was used to study the shock sensitivity of HNIW.

Results and Discussion

Supersaturation of HNIW

The solubility of HNIW was determined as described in Ref. [16]. The solubility of HNIW in ethyl acetate is 40.6 g/100 ml (average value range 10°C to 75°C). The solubility curve of HNIW is also given in Figure 2. The properties of ethyl acetate, petroleum ether and chloroform are listed in Table 1.

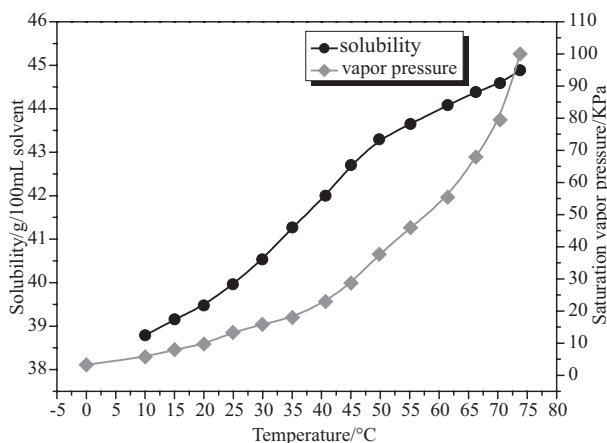


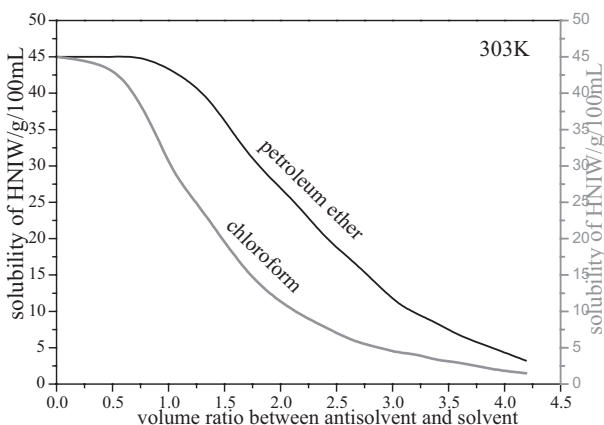
Figure 2. Solubility curve of HNIW in ethyl acetate.

Table 1. Physical properties of solvent and antisolvents

Solvent/ antisolvent	Density ρ (g·ml ⁻¹)	Viscosity @ 20 °C η (Pa·s)	Surface tension @ 20 °C σ (N·m ⁻¹)	Dipole moment p (m·C)
Ethyl acetate	0.89	0.455×10^{-3}	23.97×10^{-3}	5.94×10^{-30}
Petroleum ether	0.65	0.540×10^{-3}	20.75×10^{-3}	0
Chloroform	1.40	0.563×10^{-3}	27.97×10^{-3}	5.17×10^{-30}

During crystallization, the polarity and dipole moment of the antisolvent molecules might affect the intermolecular action in primary nucleation. Stable ϵ -HNIW could be acquired by using a non-polar or weakly polar antisolvent due to the non-reaction on the crystal surface [17]. When using ethyl acetate as the solvent, an antisolvent with a low dipole moment, for example, petroleum ether, causes HNIW to form the ϵ - modification.

For solvent-antisolvent mixtures, the solubility of HNIW measured at 30 °C is given in Figure 3.

**Figure 3.** Solubility curve of HNIW in mixed solvents.

For a given system, ethyl acetate was the solvent and petroleum ether was used as the antisolvent. The solubility of HNIW in ethyl acetate was almost constant independent of temperature (shown in Figure 2). Various volume ratios of antisolvent to solvent were used to precipitate HNIW from the saturated solution at ambient temperature. The supersaturation of HNIW solutions was mainly effected by the volume ratios of the antisolvent to solvent. Until crystal nucleation occurs in the solvent and antisolvent mixtures, the solute material (HNIW) remains in the solution. Thus, the material balance before nucleation

occurs is described by eq. 1.

$$W \frac{dC}{dt} = C \frac{dW}{dt} \quad (1)$$

As shown in eq. 1, where W and C were the weight and weight concentration of the solvent-antisolvent mixtures, respectively, t was the time scale. When the antisolvent is added to the saturated solution, the crystals cannot crystallize out instantly until the supersaturation is surpassed. For instance, before adding the antisolvent, the weight concentration of the solution was 33% defined as C_0 . With the increase of petroleum ether, the weight concentration of the mixed solution would generally reduce to C_{limited} when nucleation occurred. The volume ratio of the added petroleum ether (chloroform) to ethyl acetate was 1 (or 0.3) at the point of recrystallization. The obvious mark was also shown in Figure 3. Thus, the type and dosage of antisolvent could be chosen from the solubility of HNIW in mixtures at ambient temperature. It was found that the antisolvent addition rate had nothing to do with the supersaturation of mixtures before nucleation occurred. Crystals were obtained by a slow addition rate and the ultrafine powder was acquired by a rapid addition rate.

Structural analysis

FTIR spectra of desensitized HNIW are shown in Figure 4. The crystal form of HNIW was determined by FTIR analysis. The FTIR data were 3031 cm^{-1} (w, C—H), 1608 cm^{-1} (vs, $\nu_{\text{as}}(\text{N—NO}_2)$), 1330 cm^{-1} (s, C—C), 1285 cm^{-1} , 1260 cm^{-1} , and 1153 cm^{-1} . The FTIR spectra of HNIW obtained by recrystallization from ethyl acetate-petroleum ether mixtures and of raw HNIW are given in Figure 5. The characteristic peaks which appeared in the region of 1200 to 700 cm^{-1} were consistent with the spectrum of HNIW [18, 19]. It was demonstrated that the obvious medium quartet peaks near 740 cm^{-1} and the characteristic peak at 819.7 cm^{-1} (820.2 cm^{-1} in Ref. [16]) of HNIW in Figure 5 was almost the same as that of Ref. [18, 19]. This meant that the HNIW obtained in the solvent and antisolvent system by this recrystallization method was ϵ -HNIW. However, the percentage composition of polymorphous HNIW was not quantified by this qualitative FTIR analysis. The XRD patterns of HNIW are shown in Figure 6. There are few diffraction peaks in the patterns for α -, β -, γ -, and ϵ -HNIW above 50° . There are more than 20 diffraction peaks in each XRD pattern for α -, β -, γ -, and ϵ -HNIW, respectively, some of which are overlapping. It has been found that the ϵ -phase exhibits a unique non-overlapping diffraction peak at $19.9^\circ 2\theta$ [20]. Figure 6 shows the XRD pattern of ultrafine HNIW from 2 to $50^\circ 2\theta$.

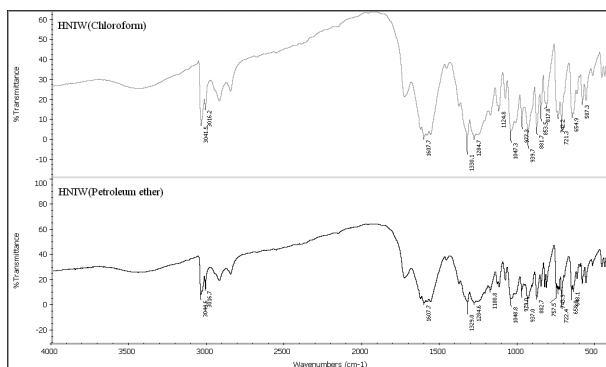


Figure 4. FTIR spectrum of HNIW recrystallized from polar and nonpolar antisolvents.

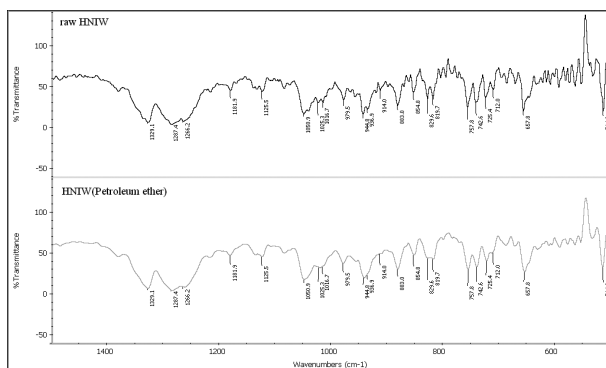


Figure 5. FTIR spectrum of D-HNIW and raw HNIW in the fingerprint region (700-1200 cm⁻¹).

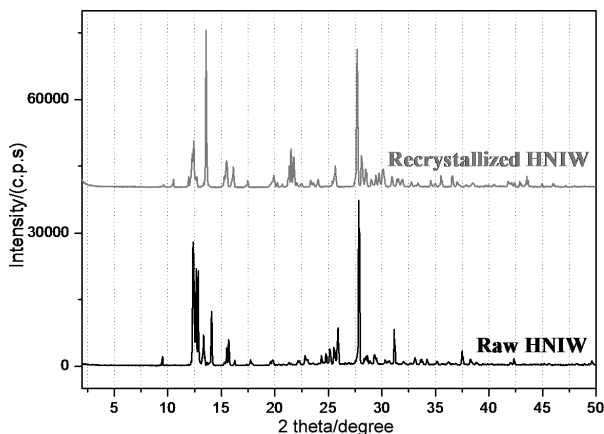


Figure 6. X-Ray diffraction patterns of raw HNIW and recrystallized HNIW.

SEM of HNIW

The SEM images of HNIW recrystallized from ethyl acetate-petroleum ether and ethyl acetate-chloroform are shown in Figure 7 (a) and 7(b), respectively. The differences in morphology between the two kinds of HNIW samples were obvious. The HNIW recrystallized from ethyl acetate-petroleum ether had a blocklike crystal morphology, with smooth and integrated particle surfaces, whereas the HNIW acquired from ethyl acetate-chloroform presented agglomerated crystallites and coarse surfaces with sharp edge angles. The crystal transformation of HNIW was mostly performed by the solvent-antisolvent method. The stability of HNIW crystals depended on their crystal morphology, i.e., ϵ -form, γ -form, α -hydrate, and β -form, and was predominantly determined by the thermodynamic conditions of temperature and solvent. When the temperature was above 70 °C, it was found that the crystal form transformed from the ϵ -form to the β -form [11]. The molecular polarity of the solvent also influenced the HNIW polymorphs during nucleation. It could be inferred that asymmetric and unstable structural polymorphs were induced by more polar solvents in the process of generating a new phase out of solution. It was possible that the γ - and α - polymorphs would appear in recrystallizations using a polar antisolvent. However, there was no doubt that the ϵ -form with a symmetric structure was obtained by using a non-polar antisolvent below 70 °C. The morphology of ϵ -HNIW shown in Figure 7(a) was almost the same as that of Ref. [6] and [21]. As a result, it was found that ϵ -HNIW grains could be prepared by the solvent-antisolvent method using non-polar solvents such as petroleum ether, *n*-heptane and cyclohexane.

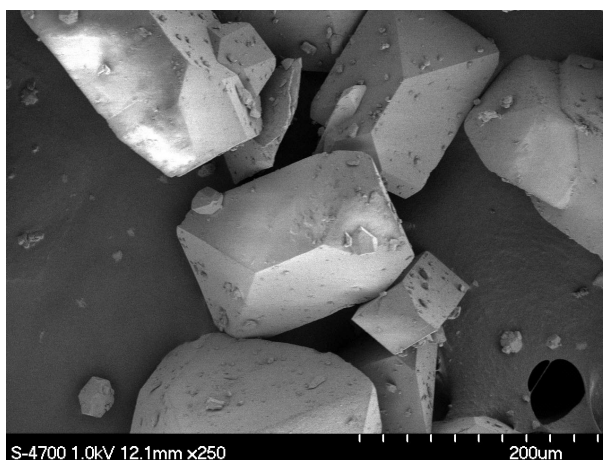


Figure 7(a). SEM image of D- ϵ -HNIW recrystallized from ethyl acetate-petroleum ether.

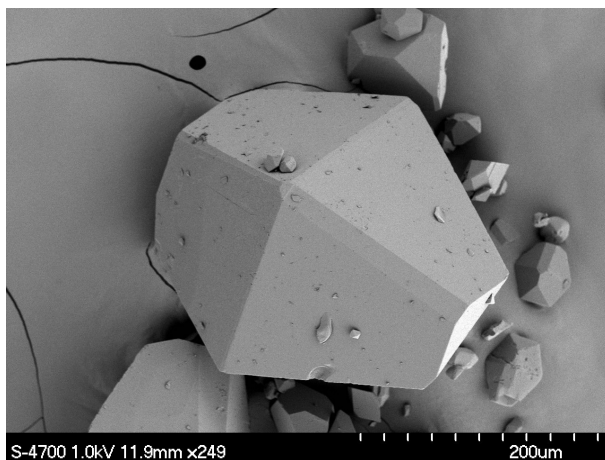


Figure 7(b). SEM image of HNIW recrystallized from ethyl acetate-chloroform.

HNIW crystals from evaporation crystallization and solvate adducts are shown in Figure 8(a) and 8(b). According to the HNIW solubility in ethyl acetate and petroleum ether mixtures (Figure 3), the 1:3.5 solvent-antisolvent volume ratio seemed to be optimum for the system with a yield of 80% (8 g/100 ml). This meant that a minimum of 20% HNIW still remained in the mother liquor. Thus it would be uneconomical to keep on adding antisolvent until completion of the crystallization. Therefore, the ethyl acetate and petroleum ether were recycled by vacuum distillation from the mother liquor. According to experimental data from Ref. [11], when the evaporation temperature was below 60 °C, the crystal density was almost independent of the evaporation rate, as the promotion of crystal growth was observed to decrease at high temperatures. At an evaporation temperature of 50 °C, the crystals had a high density of 2.02 g/cm³, with irregular morphology (steps and agglomerates) (see Figure 7(a)). The transition $\varepsilon \rightarrow \gamma$ below 64 °C was observed to be slow compared to the reverse conversion at higher temperatures [6]. The organic solvent was removed from the crystallization solution (mother liquor) while retaining the HNIW without phase transition at 50 °C. However, solvent inclusion within the HNIW crystals could not be avoided. The solvate adduct on the surface of the HNIW was introduced during crystal growth under high initial supersaturation at this temperature.

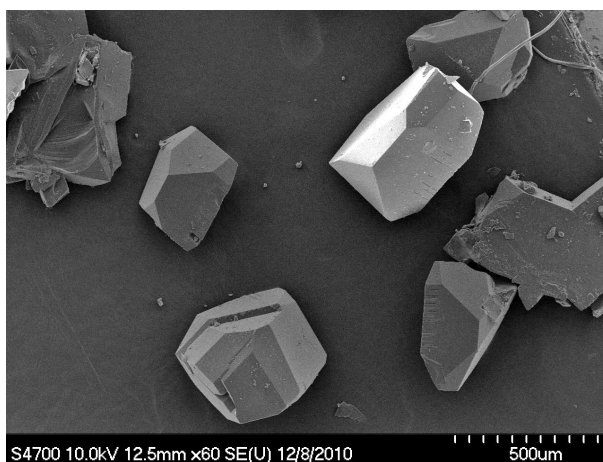


Figure 8(a). SEM image of HNIW from evaporation crystallization.

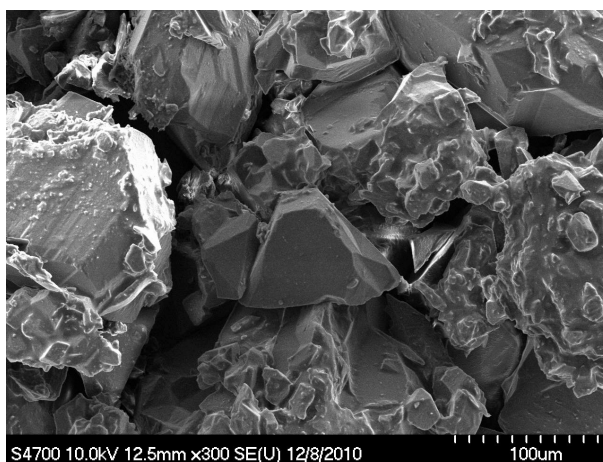


Figure 8(b). SEM image of HNIW and solvate adduct.

As shown in Figure 8(b), the viscous substance was a byproduct of carbonylnitroamine compound by evaporation crystallization at ambient temperature. Indeed, this solvate adduct was available to complex to the surface of the HNIW during slow evaporation of the mother liquor. The thermodynamic stability of the solvate adduct depended on the properties of the solvent, such as molecular weight, boiling point and polarity. In addition, it was hard to remove the solvate adduct from the surface of HNIW recrystallized by the antisolvent-solvent mixtures and this result was also confirmed by the purity test.

The HPLC results for HNIW are shown in Table 2. It was found that the

HNIW purity is 98.52% at an 80% yield via recrystallization from ethyl acetate-petroleum ether mixtures. It was unavoidable that impurity was introduced during crystallization. The impurity in HNIW was the solvate adduct. According to the data, the results still indicated that this recrystallization process for HNIW described here is suitable for ϵ -HNIW preparation.

Table 2. HPLC data of HNIW prepared by recrystallization in ethyl acetate-petroleum ether mixture

Component	Retention time (min)	Apex height (mV)	Apex area (mV·s)	Area percentage (%)
ϵ -HNIW	11.25	626.71	9359.4	98.52
solvate adduct	8.70	2.08	140.6	1.48

Thermal characteristics and sensitivity tests

The results for the DSC of the samples are shown in Figures 9(a) and 9(b). The exothermic peak at approximately 238.8 °C observed in raw HNIW (shown in Figure 9(a)), was lower than that of ϵ -HNIW (246.2 °C shown in Figure 9(b)). An endothermic response indicated that a phase transition had occurred in the HNIW. The phase transition temperature of raw HNIW was 177.5 °C (shown in Figure 9(a)), which is equal to that of ϵ -HNIW (177.6 °C). It was considered that the difference was caused by the different particle sizes and crystal polymorphs between raw HNIW and ϵ -HNIW. In the case of slow decomposition under isothermal conditions, the global kinetics for HNIW was dominated by N-NO₂ homolysis. Following the N-NO₂ homolysis, many reactions of the skeleton cage were observed. Analogous behavior was observed in HMX and RDX [22]. In the case of non-isothermal decomposition, it was considered that ϵ -HNIW exhibits almost the same reaction. As is also shown in Figure 9(b), the TG curve of ϵ -HNIW indicated similar results to that of DSC. The percentage mass loss of ϵ -HNIW was very large within a narrow temperature range (225.4-244.6 °C). The decomposition enthalpy for this temperature range showed that fast decomposition occurred in ϵ -HNIW, which was close to the decomposition enthalpy (2667 J/g) reported in Ref. [16] and was 278 J/g greater than reported by SNPE (2300 J/g). The DTG curve also showed that ϵ -HNIW had the same thermal characteristics as that described in Ref. [22]. It was clear that the first peak was derived for the initial decomposition temperature and the second peak corresponded to the maximum value. This suggested that the two peaks followed a two-step reaction mechanism in a fast decomposition of ϵ -HNIW.

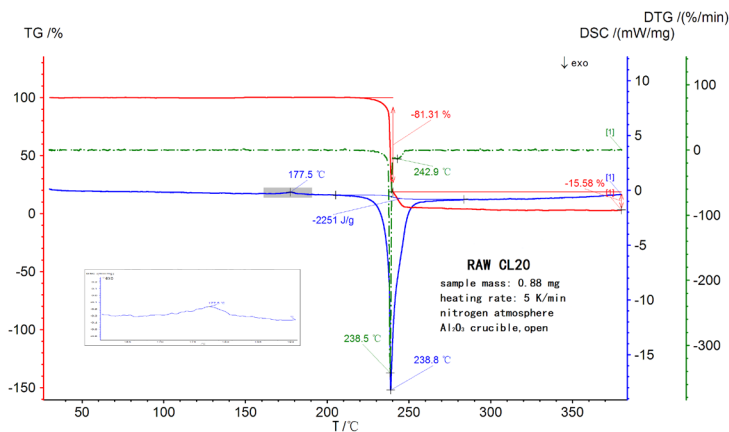


Figure 9(a). TG-DSC measurement of raw HNIW.

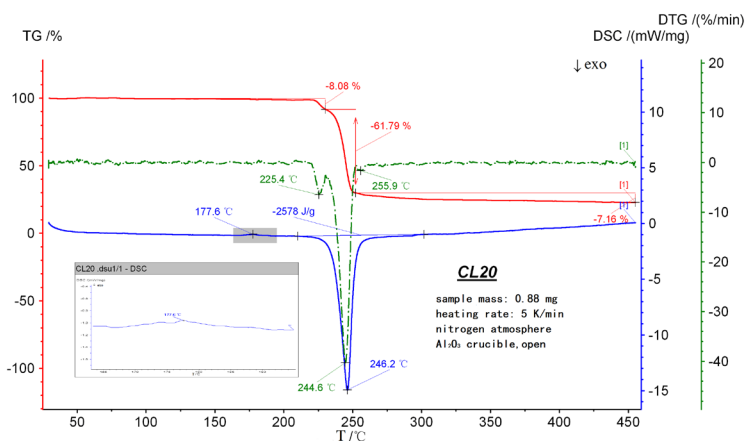
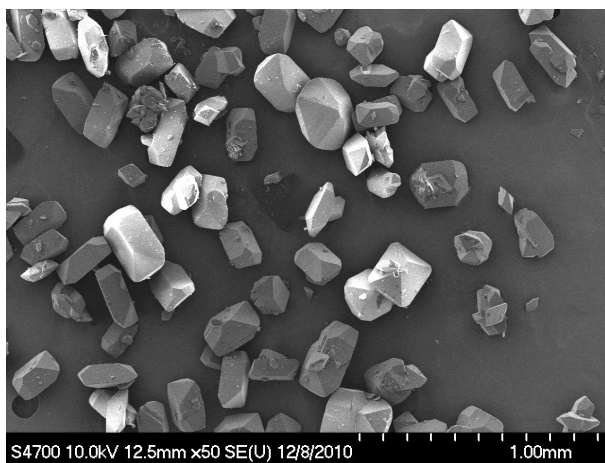
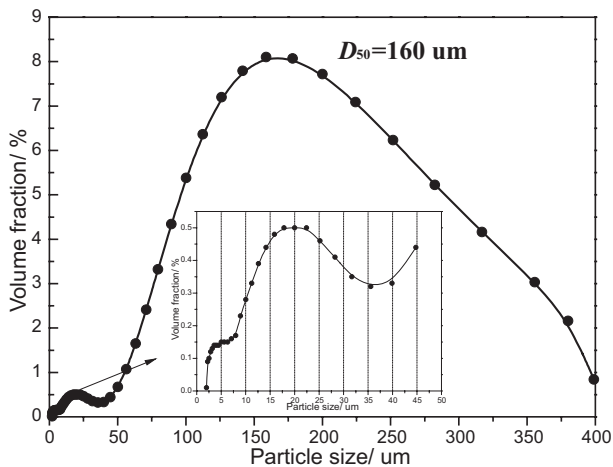


Figure 9(b). TG-DSC-DTG measurement of ϵ -HNIW.

The results of impact and friction sensitivity tests are shown in Table 3. The sensitivity, especially the impact sensitivity, was affected by the particle shape of HNIW as presented in Ref. [23-25]. The sensitivity of single crystals with regular shapes was lower than that of crystals with sharp corners. Since the particle shape of the desensitized ϵ -HNIW used in this study was regular (short column is shown in Figure 10, the particle size distribution is shown in Figure 11), this agrees with the study by J. Szczygielska et.al. [26]. The friction sensitivity of ϵ -HNIW was lower than that of RDX (5-class, SEM image is shown in Figure 12).

Table 3. Impact and friction sensitivity data of HNIW, PETN and RDX

Sample	Raw HNIW	Raw PETN	D-HNIW	RDX (5-class)
12 Tool/ H_{50} (cm)	12.8	13.6	16.8	21.8
Kast/ H_{50} (cm)	10.0	9.6	15.2	20.6
P %	100	100	60	80

**Figure 10.** SEM image of desensitized ϵ -HNIW.**Figure 11.** Particle size distribution of desensitized ϵ -HNIW.

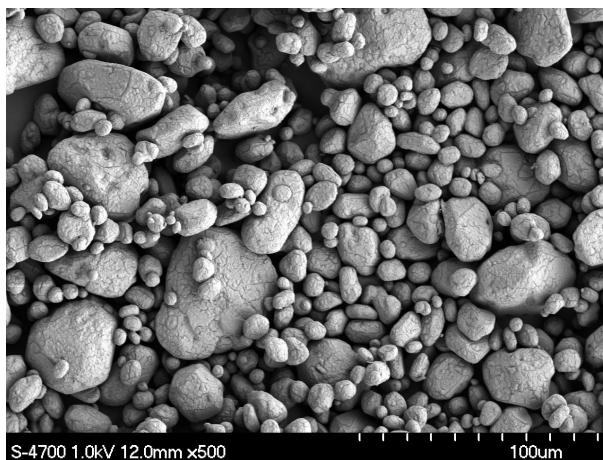


Figure 12. SEM image of 5-class RDX.

Internal crystal defects, like inclusions, may be responsible for the sensitivity of HNIW. Inclusions could act as hot spots where the shock wave initiated the reaction. If inclusions were present in HNIW crystals, this would lead to a small but generally measurable lowering of the density, since the voids were filled with solvent having a lower density than HNIW. The small scale gap test (SSGT) is one of the most general methods used to study shock wave sensitivity. The schematic diagram of the SSGT is shown in Figure 13.

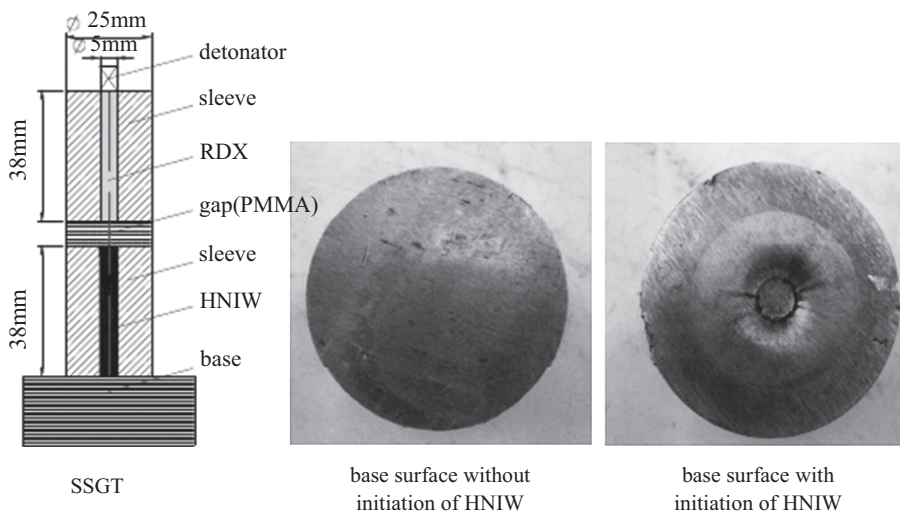


Figure 13. Small scale gap test.

The RDX (5-class) was pressed into the top sleeve; the density of the grain was 1.64 g/cm³ (90% of theoretical density). The HNIW was pressed into the lower sleeve, with 1.80 g/cm³ density (90% of theoretical density). The gap was placed between the RDX and HNIW. When the RDX was initiated by the detonator, the detonation wave propagated in the axial direction to the upper surface of the gap. The shock wave generated by the attenuating detonation wave passed through the gap. The HNIW was initiated by the shock wave penetrating the gap with a fixed thickness. If HNIW was initiated by sufficient shock wave energy, a dent would appear on the surface of the base. According to the dent depth in the base, the thickness of the gap was changed until the critical thickness was reached, when the initiation probability was 50%. The critical thickness of the gap for raw HNIW was 15.4 mm, and for desensitized ϵ -HNIW was 11.2 mm. The SSGT tests with desensitized ϵ -HNIW showed decreased sensitivity to the shock wave.

Conclusion

It was found that the crystal morphology and the density of HNIW depended on the polarity of the antisolvent, the volume ratio of antisolvent to solvent and the temperature, these being the key operating parameters in solvent-antisolvent recrystallization. Antisolvents with little or no polarity would help to form stable ϵ -HNIW with a high density. Increasing the volume ratio of the antisolvent to solvent led to a high degree of supersaturation and reduced crystal density since promoting the crystal growth process caused the formation of voids and cavities in the crystals. However, decreasing the addition rate of the antisolvent led to regular crystals with high density at the point of recrystallization. Increasing the temperature retarded the molecular sticking process of crystal growth, might cause crystal morphology transition. Ambient temperatures would ensure ideal morphology and increase the crystal density.

In addition, high supersaturation and temperature facilitated the formation of unstable crystal structures with irregular morphology; a low density powder crystallized out of solution when the volume ratio of antisolvent to solvent exceeded 1.5 (≤ 10 g magnitude) and the addition rate of the antisolvent was increased above 1 ml/min at 30 °C. Thus, desensitized ϵ -HNIW was obtained by modifying the thermodynamic conditions of the recrystallization.

References

- [1] Nielsen A.T., *Caged polynitramine compound*, US 5693794, **1997**.
- [2] Simpson R.L., Urtiew P.A., Ornellas D.L., Moody G.L., Scribner K.J., Hoffman D.M., CL-20 Performance Exceeds that of HMX and Its Sensitivity Is Moderate, *Propellants Explos. Pyrotech.*, **1997**, 22, 249-255.
- [3] Geetha M., Nair U.R., Sarwade D.B., Gore G.M., Asthana S.N., Singh H., Studies on CL-20: the Most Powerful High Energy Material, *J. Therm. Anal. Calorim.*, **2003**, 73, 913-922.
- [4] Nielsen A.T., Chafin A.P., Christian S.L., Moore D.W., Nadler M.P., Nissan R.A., Vanderah D.J., Synthesis of Polyazapolycyclic Caged Polynitramines, *Tetrahedron*, **1998**, 54, 11793-11812.
- [5] Bircher S.R., Mader P., Mathieu J., Properties of CL-20 Based High Explosives, *29th International Annual Conference of ICT*, Karlsruhe, Germany, **1998**.
- [6] Foltz M.F., Coon C.L., Garcia F., Nichols A.L., The Thermal Stability of the Polymorphs of Hexanitrohexaazaisowurtzitane, *Propellants Explos. Pyrotech.*, **1994**, 19, 19-22.
- [7] Foltz M.F., The Thermal Stability of ϵ -Hexanitrohexaazaisowurtzitane in an Estane Formulation, *Propellants Explos. Pyrotech.*, **1994**, 19, 63-65.
- [8] Sivabalan R., Gore G.M., Nair U.R., Study on Ultrasound Assisted Precipitation of HNIW and Its Effect on Morphology and Sensitivity, *J. Hazard. Mater.*, **2007**, A139, 199-203.
- [9] Patil M.N., Gore G.M., Pandit A.B., Ultrasonically Controlled Particle Size Distribution of Explosives: A Safe Method, *Ultrason. Sonochem.*, **2008**, 15, 177-187.
- [10] Bayat Y., Zeynali V., Preparation and Characterization of Nano-CL-20 Explosive, *J. Energ. Mater.*, **2011**, 29, 281-291.
- [11] Myung H.L., Jun H.K., Young C.P., Control of Crystal Density of ϵ -Hexanitrohexaazaisowurtzitane in Evaporation Crystallization, *Ind. Eng. Chem. Res.*, **2007**, 46, 1500-1504.
- [12] Borne L., Patedoye J.-C., Spycckerelle Ch., Quantitative Characterization of Internal Defects in RDX Crystals, *Propellants Explos. Pyrotech.*, **1999**, 24, 255.
- [13] Spycckerelle Ch., Eck G., Sjöberg P., Amnéus A.-M., Reduced Sensitivity RDX Obtained from Bachmann RDX, *Propellants Explos. Pyrotech.*, **2008**, 33(1), 14-19.
- [14] Bui-Dang R., Brady V., Evaluation of Reduced Sensitivity RDX in PBXN-109 in GP bomb, *35th International Annual Conference of ICT*, Karlsruhe, Germany, **2004**.
- [15] Oxley J., Smith J., Bucu R., Huang J., A Study of Reduced-sensitivity RDX, *J. Energ. Mater.*, **2007**, 25, 141-160.
- [16] Ou Y.X., *High Energetic Density Compounds* (in Chinese), 1st ed., National Defense Industry Press, Beijing, **2005**.
- [17] Jin S.H., Lei X.G., Ou Y.X., Influence of Antisolvent Property on the Modes of Crystallization of HNIW (in Chinese), *Acta Armamentarii*, **2005**, 26, 743-745.

- [18] Hakobu B., Shuichi K., Hiroshi M.Y., Synthesis and Sensitivity of Hexanitrohexaazaisowurtzitane (HNIW), *Propellants Explos., Pyrotech.*, **1998**, *23*, 333-336
- [19] Jin S.H., Shu Q.H., Chen S.S., Preparation of ϵ -HNIW by a One-Pot Method in Concentrated Nitric Acid from Tetraacetyldiformylhexaazaisowurtzitane, *Propellants Explos. Pyrotech.*, **2007**, *32*, 468-471.
- [20] Chen, H. X., Chen S. S., Li L.J., Jin S.H., Quantitative Determination of ϵ - phase in Polymorphic HNIW Using X-ray Diffraction Patterns, *Propellants Explos. Pyrotech.*, **2008**, *33*, 467-471.
- [21] Ou Y.X., Jia H.P., Chen B.-R., Research Progress of Hexanitrohexaazaisowurtzitane (3): Studies on Polymorphs of Hexanitrohexaazaisowurtzitane (in Chinese), *Chinese*, **1999**, *7*, 49-52.
- [22] Turcotte R., Vachon M., Kwok Q.S.M., Wang R., Jones D.E.G., Thermal Study of HNIW (CL-20), *Thermochim. Acta*, **2005**, *433*, 105-115.
- [23] Badgujar D.M., Talawar M.B., Asthana S.N., Advances in Science and Technology of Modern Energetic Materials: An Overview, *J. Hazard. Mater.*, **2008**, *151*, 289-305.
- [24] Nielsen A.T., Polyazapolycyclics by Condensation of Aldehydes with Amines, *J. Org. Chem.*, **1990**, *55*, 1459.
- [25] Elbeih A., Husarova A., Zeman S., Path to ϵ -HNIW with Reduced Impact Sensitivity, *Cent. Eur. J. Energ. Mater.*, **2011**, *8*(3), 173-182.
- [26] Szczygielska J., Chlebna S., Maksimowski P., Skupiński W., Friction Sensitivity of the ϵ -CL-20 Crystals Obtained in Precipitation Process, *Cent. Eur. J. Energ. Mater.*, **2011**, *8*(2), 117-130.